Received: 17 August 2022 | Revised: 21 September 2022 | Accepted: 24 September 2022

DOI: 10.1002/htj.22737

ORIGINAL ARTICLE

HEAT TRANSFER WILEY

Dual solution of heat transfer in hydromagnetic micropolar fluid flow over a stretching sheet in a porous media: A numerical approach

Mayzul A. Hussain | **Sahin Ahmed**

Department of Mathematics, Rajiv Gandhi University, Doimukh, Arunachal Pradesh, India

Correspondence
Sahin Ahmed, Department of Mathematics, Rajiv Gandhi University, Rono Hills, Doimukh, Arunachal Pradesh 791112, India.
Email: sahin.ahmed@rgu.ac.in

Abstract

In this study, the researcher looks at the heat transmission of an incompressible magneto-hydrodynamics micropolar fluid across a moving stretched surface in a Darcian permeable medium. The proper boundary conditions are used to facilitate the numerical solution (bvp4c) of the transformed governing equations. Graphical discussions have been made of the influence of the physical parameters on the velocity, angular velocity (microrotation), and temperature, and the distributions are accentuated on the plots via MATLAB. The study is validated by the previous work and it is found appropriate for investigation, where the absolute difference between the previous work and the present investigation by adopting the finite difference scheme is smaller than 10^{-5} which implies that the scheme is stable and convergent. The microrotation has a great impact on the micropolar fluid with the influences of buoyancy forces, source, and suction over the stretching surface in a Darcian regime. With a rise in the heat source parameter, both velocity and microrotational profiles lessen, but the opposite is true for temperature. Eringen number (E_r) rises with the flow velocity, whereas temperature and microrotational profiles

show the reverse relationship. The current study focused on particular applications in non-Newtonian fluid mechanics, polymer flows in filtration systems and metallurgical procedures that included cooling unbroken strips or filaments via a static fluid.

KEYWORDS

bvp4c, Darcian permeable medium, heat transmission, MHD, micropolar fluid, microrotation, stretched surface

1 | INTRODUCTION

Micropolar fluids being represented as non-Newtonian fluids are made up of microstructured polymeric additives. The fluid flow properties with heterogeneity or nonuniformity within the physical composition in a non-Newtonian fluid cannot be narrated appropriately or suitably by Navier–Stokes alone, therefore the theory of micropolar fluid projected by Eringen[1,2] came into existence and this theory allows or permits a correct model for fluid when there is a case for consideration of polymeric and rotating particles and as proposed by Eringen the problem can be overcome by involving the microrotational momentum equation together with the classical momentum equation. Theories of micropolar fluid were based on pioneering work by Eringen, Dahler, and Scriven, to name a few. Their pioneering works in the field of micropolar fluid laid the foundation for all the work done on micropolar fluid and all the works going on presently. Lately, more exploration and investigation are going on in the field of micropolar fluid by taking into consideration the physical and engineering problems moreover the examination of micropolar fluid flow received significant recognition as it fits into various applications (such as animal blood, lubricants, etc.) in industry. Numerous scholars, including Amin et al., Kartini et al., Ahmed et al., Ali et al., Mohammadein et al., Tassaddiq, and Gangadhar et al.,[3–9] investigated the magnetohydrodynamic (MHD) boundary layer of flow in micropolar fluid with the result of viscous dissipation in these papers and reported some intriguing findings. In their publications, Kalyan et al.,[10] Ishak et al.,[11] and Sheikh et al.[12] have examined the MHD micropolar fluid flow in a vertical channel. In his article, Kalyan[10] discovered that the material parameter is inversely related to fluid velocity and directly related to the microrotation velocity, while Sheikh et al.[12] found in their study that the magnetic parameter reduces the fluid velocity as well as the magnitude of microrotation, and Ishak[11] found that dual solutions exist for the assisting flow. Sui et al.[13] in their paper studied theoretically micropolar fluid flow by means of novel constitutive models in presence of heat transfer. Theoretical studies of MHD micropolar fluid flow across stretching sheets or stretchable surfaces with heat transfer were conducted by Singh et al., El-Eziz, and Yasmin et al.,[14–16] who graphically summarized the findings for the different parameters. Ahmad et al.[17] investigated micropolar fluid flow with porous media in presence of MHD in a rotating cone and the investigator found that the microrotation parameter showed decreasing behavior with the enhancement of magnetic as well as porosity parameters. The behavior of the flow of micropolar fluid under the influence of an induced magnetic field was numerically investigated by Hassan et al.,[18] and the impacts of different parameters were visually presented in the form of graphs, including the Reynold Number,

Hartmann Number, Brinkman Number, and a few other parameters. Mahmoud et al.[19] and Lavanya et al.[20] examined the impact of dissimilar physical variables on the fluid velocity, microrotation, and temperature and illustrated the impacts of these parameters on the generation of heat and thermal energy on MHD micropolar fluid flow past over stretching sheet/surface in the form of graphs. Ishak et al.[21] discovered that numerous solutions exist when the surface is going in the opposite direction from the free stream and derived similarity solutions for a flat and moving wedge plate in a fluid of microstructure. Application of magnetic drag force with a chemical reaction, Pal et al.[22] explored the effects of a periodic flow of a micropolar fluid on heat and mass transfer in a porous medium. The study found that while raising the porosity parameter of the porous medium has the opposite effect of enhancing chemical reaction, it decreases the skin-friction coefficient at the surface. To study micropolar fluid flow through a permeable inclined plate with chemical reaction in the presence of a magnetic field, Shamshuddin and Thumma[23] used numerical methods. The results showed that the mass transmission rate rose as the chemical reaction parameter increased, meanwhile the angle of inclination showed the reverse tendency. Hsiao[24] investigated the impact of radiation action on a micropolar fluid moving through a nonlinearly stretched sheet. In their study, Abbas et al.[25] examined the heat and flow exchange that occurs when a curved surface is stretched with a constant or varying surface temperature. Hazarika et al.[26–29] investigate statistically in their works how micropolar and nanofluid behave over stretchy discs and sheets in the presence of an electromagnetic field.

The importance of the study of forced/natural convection of heat transport in nanofluids under the effects of entropy generation and magnetoconvection moving in various shaped surfaces are highlighted in their investigations by Armaghani and colleagues.[30–35] Chamkha and others[36–48] have explained the impression of Hall currents, porosity, and magnetic drag forces, as well as shear, stresses over the significant fluids that contact with dissimilar surfaces under the accomplishment of buoyancy forces in connection with physical arrangements and they deliberated the worth of the outputs for the physical variations. Moreover, the consequences of micropolar fluid along a stretching sheet/disk under the application of Brownian motion and thermophoretic forces in a Darcian porous medium have enlightened in various branches of mechanical and chemical engineering and the numerical solutions have been derived by virtue of the initiation of numerical network method and bvp4c solver.[49,50]

In the current article, the researcher examined how mass and heat transmission affected the flow of a micropolar fluid when a magnetic field was present and the fluid was flowing over a constantly stretched sheet in a porous material. The set of conservation equations is transformed into ordinary differential equations by suitable transformations and is solved with help of the finite difference scheme of bvp4c. The micropolar fluid properties are investigated with the impact of physical variables over the stretching sheet.

2 | MATHEMATICAL FORMULATION

We take into account a moving stretching surface occupied in a Darcian medium, a stable two-dimensional (2D) laminar boundary layer, electrically conducting, incompressible flow, and transmission of heat of a micropolar fluid under the application of magnetic field and is presented in Figure 1. The surface is extended in the x-direction such that $U_w = ax$, where $a > 0$ is a stretching constant, is considered as the stretching velocity. A constant magnetic field B_0 in the normal direction is applied to the surface. The fluid temperatures in the free stream and close to the surface are T_w, T_∞, respectively. There is no chemical interaction between both

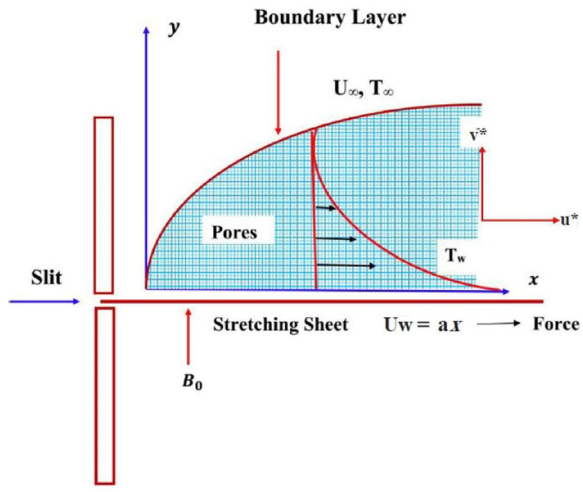

FIGURE 1 Geometry of the problem[27,29,49] [Color figure can be viewed at wileyonlinelibrary.com]

the diffusing species and the fluid in this scenario. Moreover, we assume that all fluid properties are constant.

The governing equations for fluid motion are provided below, using the boundary-layer assumptions and the aforementioned hypotheses[27,29,49]:

$$\frac{\partial u^*}{\partial x} + \frac{\partial v^*}{\partial y} = 0 \tag{1}$$

$$u^*\frac{\partial u^*}{\partial x} + v^*\frac{\partial v^*}{\partial y} = \left(\upsilon + \frac{k^*}{\rho}\right)\frac{\partial^2 u^*}{\partial y^2} + \frac{k^*}{\rho}\frac{\partial N^*}{\partial y} + \beta g(T^* - T_\infty) - \frac{\upsilon}{K_p}u^* - \frac{\sigma B_0}{\rho}u^{*2} \tag{2}$$

$$u^*\frac{\partial N^*}{\partial x} + v^*\frac{\partial N^*}{\partial y} = \frac{\gamma}{\rho j}\frac{\partial^2 N^*}{\partial y^2} - \frac{k^*}{\rho j}\left(2N^* + \frac{\partial u^*}{\partial y}\right) \tag{3}$$

$$u^*\frac{\partial T^*}{\partial x} + v^*\frac{\partial T^*}{\partial y} = \frac{k}{\rho C_p}\frac{\partial^2 T^*}{\partial y^2} - \frac{\delta^*}{\rho C_P}\left(\frac{\partial T^*}{\partial x}\frac{\partial N^*}{\partial y} + \frac{\partial T^*}{\partial y}\frac{\partial N^*}{\partial x}\right) - \frac{\gamma}{\rho C_p}(T^* - T_\infty) \tag{4}$$

The corresponding boundary conditions are[27,29,49]:

$$\left\{\begin{array}{l} y = 0: u^* = U_w = ax, v^* = V^*, N^* = \dfrac{-1}{2}\dfrac{\partial u}{\partial y}, T^* = T_w \\ y \to \infty: u^* \to 0, v^* \to 0, N^* \to 0, T^* \to T_\infty \end{array}\right\} \tag{5}$$

Here, $[u^*, v^*]$ is the velocity vector, $\nu = \frac{\mu}{\rho}$ = kinematic viscosity, μ = dynamic viscosity, ρ = density, k^* = vortex viscosity, γ = spin gradient viscosity, C_p = specific heat, T^* = temperature, j = microinertia per unit mass, N^* = microrotation, V^* = Suction velocity k = thermal conductivity of the fluid, V^* = Suction velocity and $U_w = ax$; $a > 0$ denotes the wall's velocity.

In the present study, we take the nondimensional parameters are as follows:

$$\left\{\begin{array}{l} \eta = y\left(\frac{a}{\upsilon}\right)^{1/2}, \quad \psi = (a\upsilon)^{1/2} f(\eta), \quad N^* = y\left(\frac{a^3}{\upsilon}\right)^{1/2} \Omega(\eta), \\ u^* = \frac{\partial \psi}{\partial y} = axf'(\eta), \quad v^* = -\frac{\partial \psi}{\partial x} = (a\upsilon)^{1/2} f(\eta), \quad \theta(\eta) = \frac{T^* - T_\infty}{T_w - T_\infty} \end{array}\right\} \tag{6}$$

Here, η denotes the similarity variable, ψ denotes stream function in dimensional form, $f(\eta)$ denotes the stream function in nondimensional form, $\theta(\eta)$ denotes temperature in nondimensional form, $\Omega(\eta)$ denotes microrotation in nondimensional form, and prime denotes derivation with regard to variable η.

The governing Equations (1)–(4) are converted as follows using the transformations shown in Equation (5):

$$(1 + E_r)\frac{\partial^3 f}{\partial \eta^2} + f\frac{\partial^2 f}{\partial \eta^2} - \left(\frac{\partial f}{\partial \eta}\right)^2 + G_r\theta - \frac{1}{D_a}\frac{\partial f}{\partial \eta} - M\frac{\partial f}{\partial \eta} - E_r\frac{\partial \Omega}{\partial \eta} = 0 \tag{7}$$

$$C\frac{\partial^2 \Omega}{\partial \eta^2} + C^*\left(f\frac{\partial \Omega}{\partial \eta} - G_r\frac{\partial f}{\partial \eta}\right) + E_r\left(2\Omega + \frac{\partial^2 f}{\partial \eta^2}\right) = 0 \tag{8}$$

$$\frac{1}{P_r}\frac{\partial^2 \theta}{\partial \eta^2} - f\frac{\partial \theta}{\partial \eta} - \delta\Omega\frac{\partial \theta}{\partial \eta} + \alpha\theta = 0 \tag{9}$$

And the corresponding transformed boundary conditions are:

$$\left\{\begin{array}{l} \text{At} \quad \eta = 0: \left(f = \lambda; \quad \frac{\partial f}{\partial \eta} = 1; \quad \Omega = -\frac{1}{2}\frac{\partial^2 f}{\partial \eta^2}, \quad \theta = 1\right) \\ \text{At} \quad \eta \to \infty: \left(\frac{\partial f}{\partial \eta} \to 0; \quad \Omega \to 0, \theta \to 0\right) \end{array}\right\} \tag{10}$$

where

$$\left\{\begin{array}{l} P_r = \frac{\mu C_p}{k}, E_r = \frac{k^*}{\mu}, C = \frac{\gamma \rho a}{\mu^2}, C^* = \frac{j\rho a}{\mu}, \delta = \frac{\delta^* a}{\mu C_p}, \\ \alpha = \frac{\gamma}{\mu C_p}, G_r = \frac{\rho g \beta (T_w - T_\infty)}{a^2 x}, D_a = \frac{K_p a}{\nu}, M = \frac{\sigma B_0^2}{\rho a}, \lambda = \frac{V^*}{(\mu \rho a)^{1/2}} \end{array}\right\} \tag{11}$$

The other important quantities in the physical applications are τ_w, Γ_w, and q_w which are mentioned below:

Local shear stress:

$$\tau_w = -(\mu + k)\frac{\partial u}{\partial y}\bigg]_{y=0} = -(1 + Er)\mu CRe^{1/2}\frac{\partial^2 f}{\partial \eta^2}\bigg]_{\eta=0} \tag{12}$$

Local wall couple stress:

$$\Gamma_w = \gamma \frac{\partial N}{\partial y}\bigg]_{y=0} = -\gamma Re_x\, Cx^{-1} \frac{\partial \Omega}{\partial \eta}\bigg]_{\eta=0} \tag{13}$$

Rate of heat transmission at $\eta = 0$:

$$q_w = -k_c \frac{\partial T}{\partial y}\bigg|_{y=0} = -k_c (T_w - T_\infty)\left(\frac{C}{\upsilon}\right)^{1/2} \frac{\partial \theta}{\partial \eta}\bigg|_{\eta=0} \tag{14}$$

where,

$$Re_x = \text{ Reynold's No.} = \frac{Ux}{\upsilon}$$

The expressions of $f''(0)$ and $\theta'(0)$ have been calculated as

$$C_f = \frac{\tau_w}{\rho U^2} \quad \text{and} \quad Nu_x = \frac{x q_w}{k_c (T_w - T_\infty)} \tag{15}$$

With help of (15), the following expressions are obtained:

$$C_f {Re_x}^{1/2} = -(1 + Er) \frac{\partial^2 f}{\partial \eta^2}\bigg]_{\eta=0} \tag{16}$$

$$Nu_x {Re_x}^{-1/2} = -\frac{\partial \theta}{\partial \eta}\bigg]_{\eta=0} \tag{17}$$

3 | NUMERICAL METHODS

The problem is multidimensional since it involves temperature fields, streamlines, and the geometry of the flow region is also complex, hence numerical approaches were applied for the current study. Therefore, it requires more sophisticated mathematical programming. The study has been controlled by the initial and boundary conditions and therefore, bvp4c has been adopted as numerical methods to solve the governing boundary layer equations of micropolar fluids in a porous medium.

Bvp4c is a finite difference code that implements the three-stage Lobatto IIIa formula. This is a collocation formula and the collocation polynomial provides a C^1-continuous solution that is fourth-order accurate uniformly in [a,b]. Mesh selection and error control are based on the residual of the continuous solution.

With the transformations $y(1) = f,\ y(2) = f',\ y(3) = f'', y(4) = \Omega,\ y(5) = \Omega',\ y(6) = \theta$ and $y(7) = \theta'$, where $y = [f, f', f'', \Omega, \Omega', \theta, \theta']$, the differential Equations (7)–(9) can be converted into a system of first-order ordinary differential equations

$$dydx = [y(2)$$

$$y(3)$$

$$(1 + E_r)^{-1} \times (y(2)^2 - y(1) \times y(3) - G_r \times y(6) + (1/D_a) \times y(2) + M \times y(2) + E_r \times y(5))$$

$$y(5)$$

$$(C)^{-1}((-C^*) \times (y(1) \times y(5) - G_r \times y(2)) - E_r \times (2 \times y(4) + y(3)))$$

$$y(7)$$

$$P_r \times (\delta \times y(4) \times y(7) - y(1) \times y(7) - \alpha \times y(6) - Ec \times y(3))];$$

The residual boundary conditions are

$$res = [y0(1) - \lambda; \quad y0(2) - 1; \quad y0(4) + 0.5 \times y0(3); \quad y0(6) - 1; \quad y1(2); \quad y1(4); \quad y1(6)].$$

4 | VALIDATION

The present study has been compared with the works done by Takhar et al.[48] and Zeuco et al.[49] and is found well validated with these studies. The calculated values of skin friction at various stages of the present investigation have fulfilled the criterion $|(\text{Previous work}) - (\text{present work})| < 10^{-5}$ and it asserts that the numerical calculations are stable and the scheme is convergent. Table 1 is expressed the numerical values of the skin friction $(C_f Re_x^{1/2})$ for $\alpha = 0.5$ and $\Omega = -\frac{1}{2}\frac{\partial^2 f}{\partial \eta^2} \neq 0$.

TABLE 1 Distribution of skin friction for the impact of G_r, λ, and E_r

	$\lambda = 1$			$\lambda = 3$		
G_r	$E_r = 0$	$E_r = 1$	$E_r = 3$	$E_r = 0$	$E_r = 1$	$E_r = 3$
Takhar et al.[48]						
0	1.61955	1.22475	0.87734	3.30361	2.30181	1.49237
1	1.08585	0.86335	0.66138	3.00720	2.09636	1.37355
3	0.21842	0.26595	0.27579	2.42887	1.70064	1.14047
Zueco et al.[49]						
0	1.61882	1.22387	0.87691	3.30286	2.30172	1.49210
1	1.08572	0.86326	0.66140	3.00724	2.09641	1.37360
3	0.21852	0.26587	0.27580	2.42879	1.70062	1.14050
Present investigation						
0	1.61945	1.22469	0.87726	3.30363	2.30188	1.49241
1	1.08575	0.86341	0.66140	3.00725	2.09632	1.37351
3	0.21838	0.26590	0.27583	2.42880	1.70069	1.14053

5 | RESULTS AND DISCUSSION

The results for a variety of physical parameters, including the heat source parameter, the Darcy number, the Eringen number, the magnetic parameter, and the Grashof number, are reported. The physical parametric values of micropolar fluids have been chosen with regard to the physical point of view such as the application of higher porosity and lower porosity; higher magnetic field for strong action to the fluid; higher and lower buoyancy forces; maximum and minimum suction to the surface; maximum and minimum angular rotations of the fluid. All the numerical calculations have been done via MATLAB code with respect to the default physical values otherwise stated and they are $\alpha = 0.2$, $\lambda = 0.2$, $D_a = 0.5$, $E_r = 0.5$, $M = 2$, $P_r = 0.71$, $G_r = 3$, $C = 0.5$, and $C^* = 0.3$ to plot the output of various physical properties of micropolar fluids in Darcian porous medium.

Figure 2 depicts the velocity distribution for various heat source parameter (α) values and suction parameter (λ) values of 0.5 and 0.1. In both situations, velocity falls as the heat source parameter rises. In comparison to $\lambda = 0.1$, there is a modest increase in velocity profiles for $\lambda = 0.5$. It is understood that for velocity profiles, negative values are assumed as the suction parameter decreases. Lower suction of $\lambda = 0.1$ causes molecules to move in a negative direction, creating a peak wave at $\lambda = 0.5$.

Figure 3 shows the curves of fluid temperature for disparate values of the heat source variable (α) and suction parameter (λ) = 0.1, 0.5. The temperature rises in both situations as the heat source increases. It can be observed that the temperature profiles take lower values into account when the suction parameter increases as a result of blowing. The thermal energy produced by smaller suction ($\lambda = 0.1$) raises the temperature of the fluid molecules and creates a greater loop of temperature at a larger heat source ($\alpha = 0.6$).

The effects of the heat source parameter and suction parameter, $\lambda = 0.1$ and 0.5, on microrotation are shown in Figure 4. As the heat source parameter (α) is increased, the microrotation profiles diminish. Microrotational profiles show a slight increase for $\lambda = 0.5$ compared to $\lambda = 0.1$. The microrotation is always negative, suggesting that the microelements

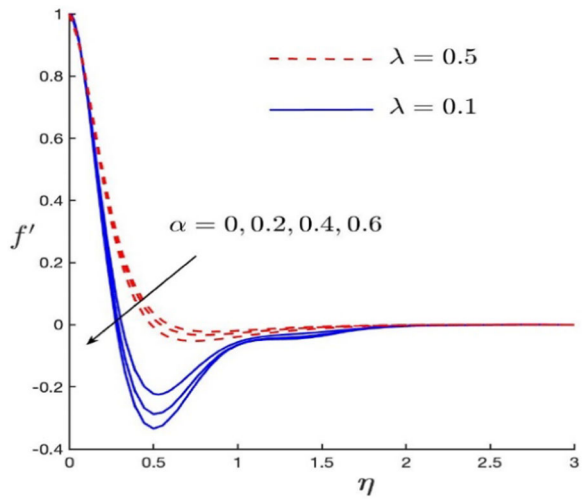

FIGURE 2 Variation of α and λ over f' [Color figure can be viewed at wileyonlinelibrary.com]

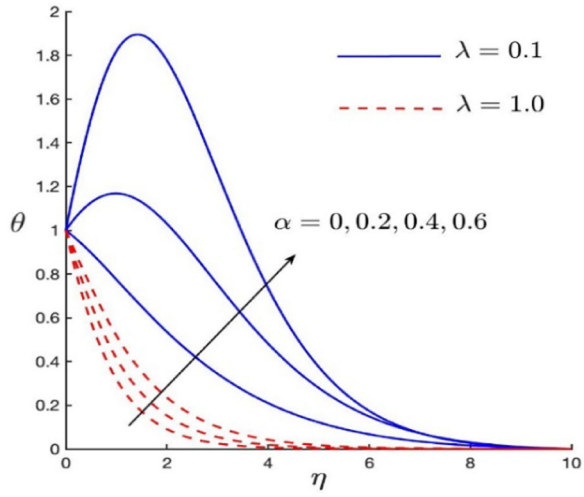

FIGURE 3 Variation of α and λ over θ [Color figure can be viewed at wileyonlinelibrary.com]

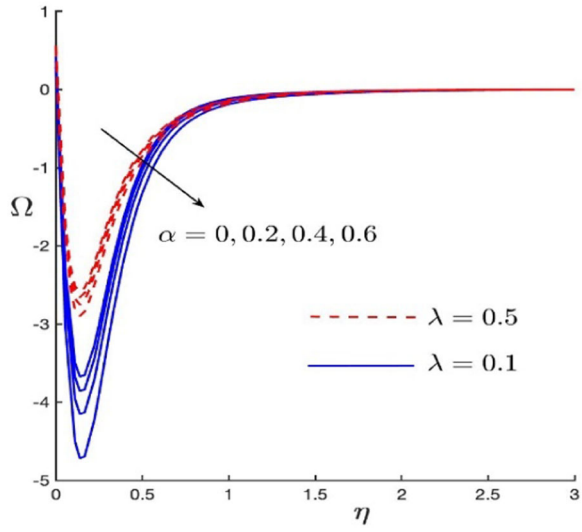

FIGURE 4 Variation of α and λ over Ω [Color figure can be viewed at wileyonlinelibrary.com]

are in a reverse spin. The amount of the microrotation upsurges near the surface as α rises, while the reverse is seen when the distance from the surface is increased.

The impact of the Eringen number (E_r) is seen in Figure 5. and $D_a = 0.1$ and infinity (∞) on velocity profiles. There is a small rise in velocity profiles for $D_a = \infty$ than for $D_a = 0.1$ accompanied by growth in Eringen number (E_r). Larger values of Eringen number (E_r) lead to an upsurge in velocity profiles.

Figure 6 depicts the impact of the application of magnetic-drag force (M) and the $E_r = 1.0, 3.0$ on temperature profiles. Along with an upsurge in M, there is a modest rise in velocity profiles for $E_r = 3.0$ compared to $E_r = 1.0$. The graph illustrates how temperature profiles rise as M rises. The temperature in the stretching sheet would rise with a rise in the

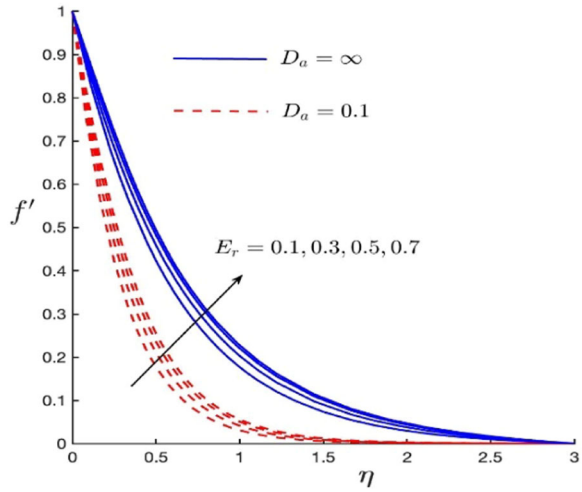

FIGURE 5 Variation of D_a and E_r over f' [Color figure can be viewed at wileyonlinelibrary.com]

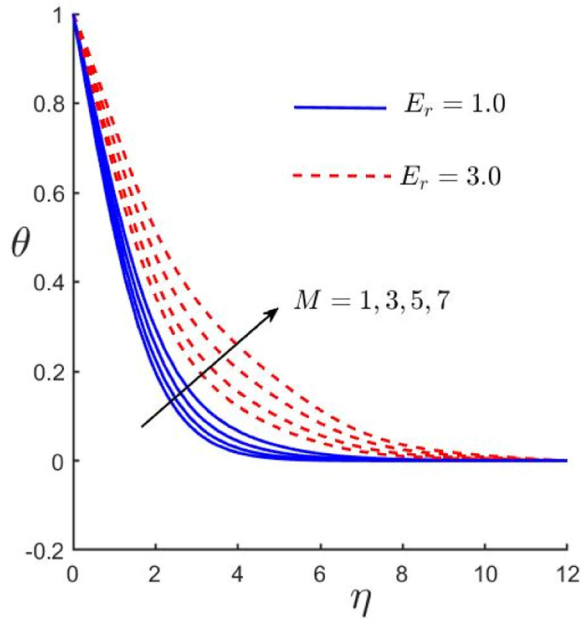

FIGURE 6 Variation of M and E_r over θ [Color figure can be viewed at wileyonlinelibrary.com]

magnetic parameter (M), as growth in M diminutions the amplitude of fluid-velocity curves caused by the Lorentz force in the stretching sheet.

The impact of the magnetic parameter (M) and $D_a = 0.1$ and infinity (∞) on the microrotation profiles is depicted in Figure 7. For $D_a = 0.1$ compared to $D_a = \infty$, there is a little increase in the microrotation profiles along with a rise in the magnetic parameter (M). Microrotation profiles grow with larger values of M. In the event of a big Darcy number $D_a = \infty$, the microrotation is always negative, showing the reverse spin of the microelements.

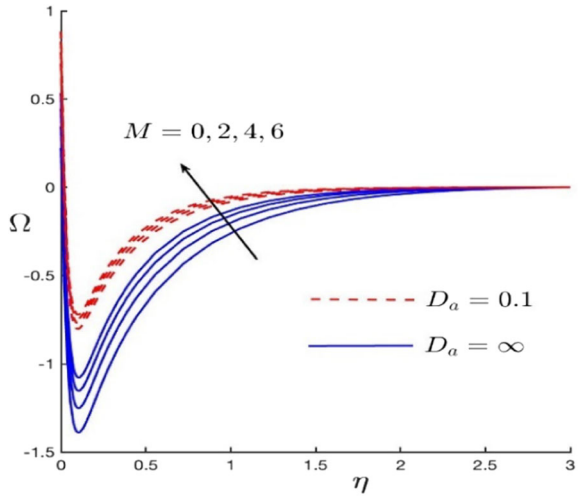

FIGURE 7 Variation of M and D_a over Ω [Color figure can be viewed at wileyonlinelibrary.com]

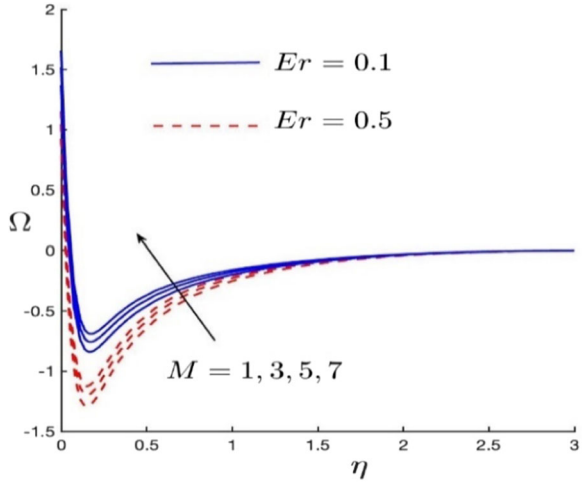

FIGURE 8 Variation of M and E_r over Ω [Color figure can be viewed at wileyonlinelibrary.com]

As M rises, the microrotation's magnitude rises close to the surface, but further from the surface, the reverse is seen.

The impact of the magnetic parameter (M) and $E_r = 0.1$ and 0.5 on the microrotation profiles is depicted in Figure 8. When $E_r = 0.1$ instead of $E_r = 0.5$, there is a little rise in the microrotation profiles along with an intensification in the magnetic parameter (M). Microrotation profiles grow as the magnetic parameter (M) rises. The microrotation is always negative, suggesting that the microelements are in reverse spin. Near the surface, the magnitude of the microrotation grows as M rises, but farther from the surface, the reverse is seen.

The impact of the magnetic parameter (M) and $Gr = 0.2$ and 2.0 on the microrotation profiles is depicted in Figure 9. Microrotation patterns somewhat differ between $Gr = 2.0$ and $Gr = 0.2$, and the magnetic parameter (M) also increases. Microrotation profiles grow with

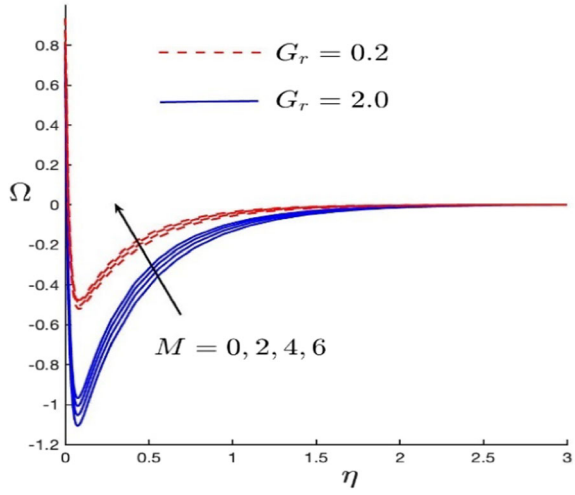

FIGURE 9 Variation of M and G_r over Ω [Color figure can be viewed at wileyonlinelibrary.com]

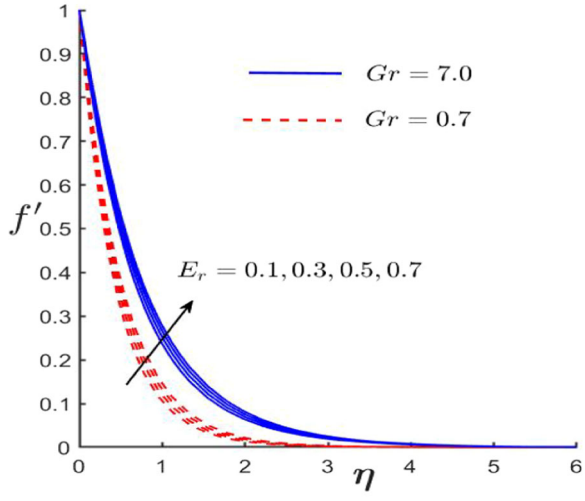

FIGURE 10 Variation of G_r and E_r over f' [Color figure can be viewed at wileyonlinelibrary.com]

larger values of M. The microrotation is always negative, suggesting that the microelements are in reverse spin. The size of the microrotation rises as M grows close to the surface, whereas the reverse is seen farther away from the surface.

The impact of the Eringen number (E_r) is seen in Figure 10 and $G_r = 7.0$ and 0.7 on velocity profiles. There is a small increase in velocity profiles for $G_r = 7.0$ than for $G_r = 0.7$ accompanied by increase in Eringen number (E_r). Larger values of E_r lead to an increase in velocity profiles. Buoyancy forces have a tendency to overshoot the velocity of the molecules opposite to the direction of acceleration due to gravity due to the change of density variation and thus the molecules of micropolar fluid have a higher velocity for the greater impact of $G_r = 7.0$ than the smaller $G_r = 0.7$.

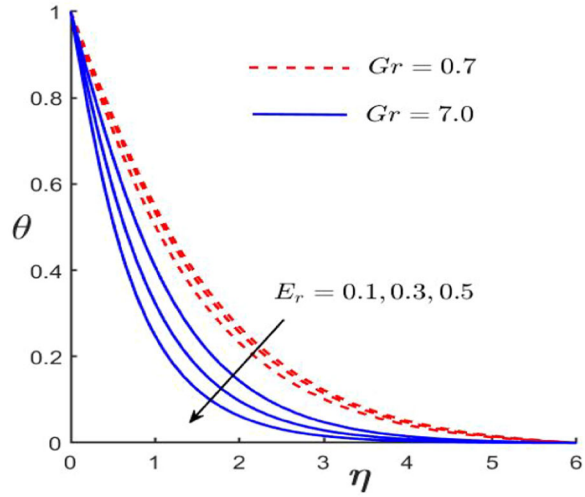

FIGURE 11 Variation of G_r and E_r over θ [Color figure can be viewed at wileyonlinelibrary.com]

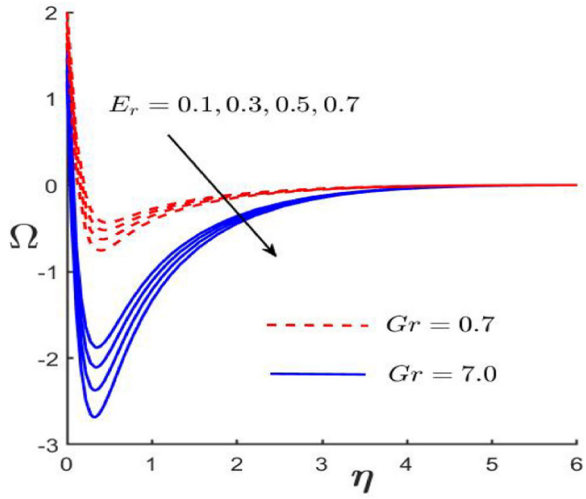

FIGURE 12 Variation of G_r and E_r over Ω [Color figure can be viewed at wileyonlinelibrary.com]

Figure 11 depicts the effect of Eringen number (E_r) and $G_r = 0.7$ and 7.0 on the curves of fluid temperature (θ). Small declination has been marked in θ for $G_r = 7.0$ than for $G_r = 0.7$ accompanied by an increase in Eringen number (E_r). There is a declination in temperature profiles for higher values of the Eringen number. The application of higher buoyancy forces over the temperature performances opposite to the velocity of molecules due to temperature differences and thus higher G_r suppresses the fluid temperature and the lower G_r augments the temperature.

Figure 12 depicts the effect of Eringen number (E_r) and $G_r = 0.7$ and 7.0 on microrotation profiles. There is a small decline in microrotation profiles for $G_r = 7.0$ than for $G_r = 0.7$ accompanied by an increase in Eringen number (E_r). There is declination in temperature profiles for higher values of the Eringen number. The microrotation is always negative,

suggesting that the microelements are in reverse spin. The strength of the microrotation rises as E_r grows close to the surface, whereas the reverse is seen farther away from the surface.

6 | CONCLUSIONS

The purpose of the current research is to investigate how mass and heat transfer affect the MHD micropolar fluid flow through a constantly moving stretched sheet in a porous material. The effects of various factors on temperature, microrotation, and velocity are discussed. The following are the key conclusions drawn from the current work:

1. Flow velocity diminishes with an increase in heat source parameter (α), whereas increases with an increase in Eringen number (E_r).
2. Intensifications in the magnetic-drag force (M) and heat source variable (α) both cause a rise in temperature, whereas increases in the Eringen number (E_r) cause a reduction in temperature.
3. When the heat source parameter and the Eringen number (E_r) are increased, angular momentum (microrotation) decreases but it increases when the magnetic parameter (M) is increased.
4. Microrotation causes the micropolar fluid to spin more strongly in the negative direction.
5. Asymptotic solutions have occurred over the momentum, the thermal and angular momentum of the molecules.
6. Instead of the lower Darcy, the higher Darcy impacts the flow velocity, which increases the mobility of molecules.
7. Table 1 shows that the shear stresses ($C_f Re_x^{1/2}$) are declined with the augmentation of forces of buoyancy forces and Eringen in the micropolar fluid by the application of suction (λ).
8. The practical application of the current work is in polymer technology, which involves stretching plastic sheets.

NOMENCLATURE

B_0	magnetic induction (Tesla)
C_p	specific heat ($Jkg^{-1}K^{-1}$)
D_a	Darcy number
U_w	wall's velocity (ms^{-1})
V^*	suction velocity (ms^{-1})
N^*	microrotation (s^{-1})
μ	dynamic viscosity (Pa.s)
ν	kinematic viscosity (m^2s^{-1})
K_p	permeability of porous medium,
k^*	vortex viscosity
ρ	density of micropolar fluid (kgm^{-3})
γ	spin gradient viscosity coefficient (Pa.s)
δ^*	micropolar heat conduction coefficient
E_r	Eringen micropolar number
δ	heat conduction parameter
G_r	Grashof number
M	magnetic parameter

α heat source parameter
λ constant suction parameter
m^2 C and C^* are constants
β volume coefficient expansion (K^{-1})
σ fluid electrical conductivity (Sm^{-1})

DATA AVAILABILITY STATEMENT

Data sharing is not applicable to this article.

REFERENCES

1. Eringen AC. Theory of micropolar fluids. *J Math Mech*. 1966;16:1-18.
2. Eringen AC. Theory of thermomicrofluids. *J Math Anal Appl*. 1972;38:480-496. doi:10.1016/0022-247X(72)90106-0
3. El-Amin MF, Mohammadein AA. Effects of viscous dissipation and joule heating on magnetohydrodynamic hiemenz flow of a micropolar fluid. *Heat Transfer Engineering*. 2005;26:75-81. doi:10.1080/01457630590951168
4. Ahmad K, Ishak A, Nazar R. Micropolar fluid flow and heat transfer over a nonlinearly stretching plate with viscous dissipation. *Math Prob Eng*. 2013;2013:1-5. doi:10.1155/2013/257161
5. Mohammadein AA, Gorla RSR. Heat transfer of a micropolar fluid over a stretching sheet with a viscous dissipation and internal heat generation. *Int J Num Method Heat Fluid Flow*. 2001;11:50-58. doi:10.1108/09615530110364088
6. Ahmad S, Ashraf SM, Ali K. Numerical simulation of viscous dissipation in a micropolar fluid flow through a porous medium. *J Appl Mech Tech Phys*. 2019;60:996-1004. doi:10.1134/S0021894419060038
7. Lund LA, Omar Z, Khan I, Raza J, Sherif EM, Seikh AH. Magnetohydrodynamic (MHD) flow of micropolar fluid with effects of viscous dissipation and joule heating over an exponential shrinking sheet: triple solutions and stability analysis. *Symmetry*. 2020;12:1-16. doi:10.3390/sym12010142
8. Tassaddiq A. Impact of Cattaneo-Christov heat flux model on MHD hybrid nano-micropolar fluid flow and heat transfer with viscous and joule dissipation effects. *Sci Rep*. 2021;11:1-14. doi:10.1038/s41598-020-77419-x
9. Gangadhar K, Kumar S, Narayana KL, Subhakar MJ, Kumar BR. Effect of viscous dissipation of a magneto hydrodynamic micropolar fluid with momentum and temperature dependent slip flow. *Mater Sci Eng*. 2017;263:1-19. doi:10.1088/1757-899X/263/6/062011
10. Kalyan S, Sharan A, Jyothi S. Effect of material parameter on mixed convective fully developed micropolar fluid flow in a vertical channel. *Heat Transfer*. 2021;50:5853-5864. doi:10.1002/htj.22152
11. Ishak A, Nazar R, Pop I. Magnetohydrodynamics (MHD) flow of a micropolar fluid towards a stagnation point on a vertical surface. *Comput Math Appl*. 2008;56:3188-3194. doi:10.1016/j.camwa.2008.09.013
12. Sheikh NA, Ali F, Khan I, Saqib M, Khan A. MHD flow of micropolar fluid over an oscillating vertical plate embedded in porous media with constant temperature and concentration. *Math Prob Eng*. 2017;2017:1-20. doi:10.1155/2017/9402964
13. Sui J, Zhao P, Cheng Z, Zheng L, Zhang X. A novel investigation of a micropolar fluid characterized by nonlinear constitutive diffusion model in boundary layer flow and heat transfer. *Phys Fluids*. 2017;29:1-10. doi:10.1063/1.4976642
14. Singh K, Pandey AK, Kumar M. Numerical solution of micropolar fluid flow via stretchable surface with chemical reaction and melting heat transfer using Keller-Box method. *Propul Power Res*. 2021;10:194-207. doi:10.1016/j.jppr.2020.11.006
15. Aziz MAE. Viscous dissipation effect on mixed convection flow of a micropolar fluid over an exponentially stretching sheet. *Can J Phys*. 2009;87:359-368. doi:10.1139/P09-047
16. Yasmin A, Ali K, Ashraf M. Study of heat and mass transfer in MHD flow of micropolar fluid over a curved stretching sheet. *Sci Rep*. 2020;10:1-11. doi:10.1038/s41598-020-61439-8

17. Ahmad Ali SK, Bashir H. Interaction of micropolar fluid structure with the porous media in the flow due to a rotating cone. *Alex Eng J*. 2021;60:1249-1257. doi:10.1016/j.aej.2020.10.048
18. Ismail HNA, Abourabia AM, Hammad DA, Ahmed NA, Desouky AAE. On the MHD flow and heat transfer of a micropolar fluid in a rectangular duct under the effects of the induced magnetic field and slip boundary conditions. *SN Appl Sci*. 2020;2:25. doi:10.1007/s42452-019-1615-9
19. Mahmoud MAA, Waheed SE. MHD flow and heat transfer of a micropolar fluid over a stretching surface with heat generation (absorption) and slip velocity. *J Egypt Math Society*. 2012;20:20-27. doi:10.1016/j.joems.2011.12.009
20. Lavanya B, Ratnam AL. The effects of thermal radiation, heat generation, viscous dissipation and chemical reaction on MHD micropolar fluid past a stretching surface in a non-Darcian porous medium. *Global J Eng Design Technol.* 2014;3:28-40.
21. Ishak A, Nazar R, Pop I. Moving wedge and flat plate in a micropolar fluid. *Int J Eng Sci*. 2006;44:1225-1236. doi:10.1016/J.IJENGSCI.2006.08.005
22. Pal D, Biswas S. Perturbation analysis of magnetohydrodynamics oscillatory flow on convective-radiative heat and mass transfer of micropolar fluid in a porous medium with chemical reaction. *Eng Sci Tech.* 2016;19:444-462. doi:10.1016/j.jestch.2015.09.003
23. Shamshuddin MD, Thumma T. Numerical study of a dissipative micropolar fluid flow past an inclined porous plate with heat source/sink. *Propul Power Res*. 2019;8:56-68. doi:10.1016/j.jppr.2019.01.001
24. Hsiao KL. Heat and mass transfer for micropolar flow with radiation effect past a nonlinearly stretching sheet. *Heat Mass Transfer*. 2010;46:413-419. doi:10.1007/s00231-010-0580-z
25. Abbas Z, Naveed M, Sajid M. Heat transfer analysis for stretching flow over curved surface with magnetic field. *J Eng Ther Phy.* 2013;22:337-345. doi:10.1134/S1810232813040061
26. Hazarika S, Ahmed S. Material behaviour in micropolar fluid of brownian motion over a stretchable disk with application of thermophoretic forces and diffusion-thermo. *J Naval Architect Mar Eng*. 2021;18:25-38. doi:10.3329/jname.v18i1.52518
27. Hazarika S, Ahmed S, Chamkha AJ. Investigation of nanoparticles cu, ag and Fe_3O_4 on thermophoresis and viscous dissipation of MHD nanofluid over a stretching sheet in a porous regime: A numerical modelling. *Math Comput Simul*. 2021;182:819-837. doi:10.1016/j.matcom.2020.12.005
28. Hazarika S, Ahmed S. Steady magnetohydrodynamic micropolar casson fluid of brownian motion over a solid sphere with thermophoretic and buoyancy forces: numerical analysis. *J Nanofluids*. 2020;9:336-345. doi:10.1166/jon.2020.1752
29. Hazarika S, Ahmed S. Impact of thermal conductivity on a horizontal absorbent isothermal wall in porous medium with heat source and thermophoretic forces: application of Suction/Blowing. *Heat Transfer J*. Published online August 19, 2022:1-18. doi:10.1002/htj.22676
30. Armaghani T, Esmaeili H, Mohammadpoor YA, Pop I. MHD mixed convection flow and heat transfer in an open c-shaped enclosure using water-copper oxide nanofluid. *Heat Mass Transfer*. 2018;54(6):1791-1801. doi:10.1007/s00231-017-2265-3
31. Armaghani T, Chamkha AJ, Rashad AM, Mansour MA. Inclined magneto: convection, internal heat, and entropy generation of nanofluid in an I-shaped cavity saturated with porous media. *J Thermal Anal Calor*. 2020;142(6):2273-2285. doi:10.1007/s10973-020-09449-6
32. Hussain S, Armaghani T, Jamal M. Magnetoconvection and entropy analysis in t-shaped porous enclosure using finite element method. *J Thermophys Heat Transfer.* 2019;34(1):203-214. doi:10.2514/1.T5821
33. Sadeghi MS, Anadalibkhah N, Ghasemiasl R, et al. On the natural convection of nanofluids in diverse shapes of enclosures: an exhaustive review. *J Thermal Anal Calor*. 2020;147(1):1-12. doi:10.1007/s10973-020-10222-y
34. Ayoubloo KA, Ghalambaz M, Armaghani T, Noghrehabadi A. Pseudoplastic natural convection flow and heat transfer in a cylindrical vertical cavity partially filled with a porous layer. *Int J Num Methods Heat Fluid Flow*. 2019;30(3):1096-1114. doi:10.1108/HFF-06-2019-0464
35. Saryazdi AB, Talebi F, Armaghani T, Pop I. Numerical study of forced convection flow and heat transfer of a nanofluid flowing inside a straight circular pipe filled with a saturated porous medium. *Eur Phys J Plus*. 2016;131(4):1-11. doi:10.1140/epjp/i2016-16078-6
36. Chamkha AJ. MHD-free convection from a vertical plate embedded in a thermally stratified porous medium with Hall effects. *Appl Math Model*. 1997;21(10):603-609. doi:10.1016/S0307-904X(97)00084-X

37. Krishna MV, Chamkha AJ. Hall and ion slip effects on MHD rotating boundary layer flow of nanofluid past an infinite vertical plate embedded in a porous medium. *Results Phys*. 2019;15:102652. doi:10.1016/j.rinp.2019.102652
38. Krishna MV, Ahamad NA, Chamkha AJ. Hall and ion slip effects on unsteady MHD free convective rotating flow through a saturated porous medium over an exponential accelerated plate. *Alex Eng J*. 2020;59(2):565-577. doi:10.1016/j.aej.2020.01.043
39. Chamkha AJ, Ben-Nakhi A. MHD mixed convection-radiation interaction along a permeable surface immersed in a porous medium in the presence of soret and Dufour's effects. *Heat Mass Transfer*. 2008;44:845-856. doi:10.1007/s00231-007-0296-x
40. Chamkha AJ. Non-Darcy fully developed mixed convection in a porous medium channel with heat generation/absorption and hydromagnetic effects. *Num Heat Transfer A Appl*. 1997;32(6):653-675. doi:10.1080/10407789708913911
41. Kumar KG, Reddy MG, Sudharani MVVNL, Shehzad SA, Chamkha AJ. Cattaneo-Christov heat diffusion phenomenon in Reiner-Philippoff fluid through a transverse magnetic field. *Phys A Stat Mech Appl*. 2020;541:123330. doi:10.1016/j.physa.2019.123330
42. Magyari E, Chamkha AJ. Combined effect of heat generation or absorption and first-order chemical reaction on micropolar fluid flows over a uniformly stretched permeable surface: the full analytical solution. *Int J Therm Sci*. 2010;49(9):1821-1828. doi:10.1016/j.ijthermalsci.2010.04.007
43. Takhar HS, Chamkha AJ, Nath G. MHD flow over a moving plate in a rotating fluid with magnetic field, hall currents and free stream velocity. *Int J Eng Sci*. 2002;40(13):1511-1527. doi:10.1016/S0020-7225(02)00016-2
44. Chamkha AJ. Hydromagnetic three-dimensional free convection on a vertical stretching surface with heat generation or absorption. *Int J Heat Fluid Flow*. 1999;20(1):84-92. doi:10.1016/S0142-727X(98)10032-2
45. Chamkha AJ, Al-Mudhaf AF, Pop I. Effect of heat generation or absorption on thermophoretic free convection boundary layer from a vertical flat plate embedded in a porous medium. *Int. Commun Heat Mass Transfer*. 2006;33(9):1096-1102. doi:10.1016/j.icheatmasstransfer.2006.04.009
46. Modather M, Rashad AM, Chamkha AJ. An analytical study of MHD heat and mass transfer oscillatory flow of a micropolar fluid over a vertical permeable plate in a porous medium. *Turkish J Eng Env Sci*. 2009;33:245-257. doi:10.3906/muh-0906-31
47. Chamkha AJ. Thermal radiation and buoyancy effects on hydromagnetic flow over an accelerating permeable surface with heat source or sink. *Int J Eng Sci*. 2000;38(15):1699-1712. doi:10.1016/S0020-7225(99)00134-2
48. Takhar HS, Agarwal RS, Bhargava R, Jain S. Mixed convection flow of a micropolar fluid over a stretching sheet. *Heat MassTransf*. 1998;34:213-219.
49. Zueco J, Ahmed S, López-Ochoa LM. Magneto-Micropolar flow over a stretching surface embedded in a darcian porous medium by the numerical network method. *Arab J Sci Eng*. 2014;39:5141-5151. doi:10.1007/s13369-014-1175-7
50. Hazarika S, Ahmed S. Material behaviour in micropolar fluid of brownian motion over a stretchable disk with application of thermophoretic forces and diffusion-thermo. *J Naval Architect Marine Eng*. 2021;18(1):25-38. doi:10.3329/jname.v18i1.52518

How to cite this article: Hussain MA, Ahmed S. Dual solution of heat transfer in hydromagnetic micropolar fluid flow over a stretching sheet in a porous media: a numerical approach. *Heat Transfer*. 2022;1-17. doi:10.1002/htj.22737